FAU Institutional Repository

http://purl.fcla.edu/fau/fauir

This paper was submitted by the faculty of FAU's Harbor Branch Oceanographic Institute.

Notice: ©1993 IEEE. Personal use of this material is permitted. Permission from IEEE must be obtained for all other uses, in any current or future media, including reprinting/republishing this material for advertising or promotional purposes, creating new collective works, for resale or redistribution to servers or lists, or reuse of any copyrighted component of this work in other works.

This manuscript is available at http://ieeexplore.ieee.org/ and may be cited as: Yu, C.-H., & Caimi, F. M. (1993). Determination of horizontal motion through optical flow computations. *Oceans '93: Engineering in harmony with the ocean: proceedings*. (Vol. 2, pp. 475-480). New York, N.Y: Institute of Electrical and Electronics Engineers. doi:10.1109/OCEANS.1993.326142

Determination of Horizontal Motion through Optical Flow Computations

Chih-Ho Yu *Frank M. Caimi*

Harbor Branch Oceanographic Institution, Inc.
5600 US 1 North
Fort Pierce, Florida 34946

Abstract - **Accurate navigation (localization) is one of the most essential capacities for an intelligent/autonomous subsea vehicle. For many applications, reliable short-range horizontal positioning is difficult to achieve, particularly over flat bottom topography. A potential solution to this problem proposed in this paper utilizes a passive optical sensing method (optical flow computation) to estimate the vehicle displacement using the bottom surface texture. Fundamentally, the proposed method is similar to correlation methods. However, it is computationally more efficient than correlation methods since it avoids blind searching a large neighbor region. The proposed method does not require feature correspondences in images and is robust in allowing brightness changes between image frames.**

I. INTRODUCTION

There are many applications of unmanned vehicles in marine field. Remotely operated vehicles are an important tool for many undersea operations. During long duration surveys, operator fatigue and inattention are major factors influencing the reliability of remote operations. Safety, flexibility and economics are other major factors that dictate the need for the development of undersea vehicles with a great degree of autonomy.

It is obvious that one of the most essential capabilities for an intelligent/autonomous subsea vehicle is accurate positioning and localization. Determining accurate orientation, that is, the roll, pitch, and yaw, can be achieved using gyroscopes while accurate depth sensing is possible using pressure sensors. Long to medium range positioning can be achieved using sonar. Scanning-laser technology has offered increased information content and data rate with better angular resolution. Ultrashort-, short-, and long-baseline acoustic sensing are well-developed, providing positional accuracy of 5-10 meters at a distance of a few kilometers, to about one meter at a few hundred meters. With the support of a mother-ship, an accuracy of a few centimeters is possible for a baseline of hundred meters. For short-range sensing, positioning can be done via acoustic or optical beacons that are placed on the ocean floor. In this application, optical sensing offers the advantage of a higher data rate, at the expense of a lower range. Active optical sensing, such as structured light methods, developed for land-based systems can be employed for increased data rate and higher resolution in comparison to acoustic ranging. However, such methods require frequent sampling to obtain accurate information about the tilt angle of the scene surface to compute the vehicle displacement.

For many applications, reliable short-range horizontal positioning is rather difficult to achieve, particularly over flat bottom topography. For example, doppler acoustic methods using dead reckoning are subject to significant drift. Other inertial navigation systems using accelerometers suffer from the same drawback since horizontal displacement is obtained by performing a double integration with respect to time. A potential solution proposed in this paper utilizes a passive optical sensing method to estimate the vehicle displacement using the bottom surface texture.

The proposed method determines horizontal motions using the optical flow technique. The method does not require feature correspondences in images and is robust in allowing brightness changes between image frames. Fundamentally, this method is similar to using correlation to match images and compute the motion disparity. However, the proposed method is computationally efficient because it avoids the blind searching of neighboring region that is required with correlation algorithms. Furthermore, the use of optical flow techniques appears to provide more robust than correlation especially when the image brightness is too random to correlate or image brightness changes. The advantages of the proposed method have been verified by our experiments.

In this paper, we first briefly introduce the concept of optical flow and then discuss optical flow computations in discrete form for digital computer implementation. Particularly, we will investigate a least squares solution. An error analysis shows that optical flow is erroneous except for null motion. Based on this, we suggest an iterative shifting method to accurately determine motion. Results from recent experiments are presented.

II. OPTICAL FLOW

Relative motion between a camera and its imaged scene can be determined from the variation of image brightness patterns, the so-called optical flow. Computing optical flow with an acceptable error, even in land environments, is a difficult problem and has been studied extensively.

Let $E(x, y, t)$ denote the image brightness of an imaged point p in the scene. At time $t + \delta t$, the scene point may be imaged onto a new location $(x + x_t\delta t, y + y_t\delta t)$ in the image due to the relative motion between the camera and scene. The body of research on optical flow usually assumes that, in the absence of other scene events, the brightness of a surface patch remains relatively constant as the surface moves in the environment relative to the viewer. This is the so-called *brightness constancy assumption* [1], which can be written as

$$E(x + x_t\delta t, y + y_t\delta t, t + \delta t) = E(x, y, t). \quad (1)$$

0-7803-1385-2/93/$3.00 © 1993 IEEE

This model is exact under several conditions: (1) (spatially) stationary and (temporally) invariant illumination; (2) stationary rigid scene (only camera motion is allowed); and (3) pure Lambertian surface of the scene. If motion of imaged objects is allowed, the motion cannot be rotational and the illumination must be uniform. Therefore, brightness constancy is not a good model in many applications where brightness variations due to nonuniform illumination, cast shadows, changes in the reflectance of the surface or irradiance gain due to interreflection and so on. For example, machine vision systems for undersea applications cannot satisfy these brightness constancy conditions. Sun light attenuates significantly in natural waters [2] and can hardly reach more than 30 meters below the water surface [3]. Therefore, artificial lighting is necessary for optical imaging in deep sea. It is obvious that images taken by divers or underwater robots moving in the sea with a self-contained light source are not suitable for using brightness constancy assumption.

Several models (e.g. [4], [5], [6]) are suggested to relax the brightness constancy. A quite general model proposed in [6] is

$$E(x+x_t\delta t, y+y_t\delta t, t+\delta t) = (1+\delta m)E(x,y,t)+\delta c. \quad (2)$$

This model attempts to incorporate effects from any event that changes the image brightness of a point through a linear transformation. For example, if image brightness is modeled as the product of an illumination field and the surface reflectance field, changes in illumination can be captured by the multiplier field δm. Other examples include applications of a sensor with computer-controlled aperture or exposure time to optimize image quality, to maintain a steady average brightness level, to prevent camera saturation, or to increase signal-to-noise ratio when illumination drops. In comparison, variations in irradiance gain due to interreflection or specular reflection, as well as saturation of the sensor in the dark or bright regions of the image due to large increase or decrease in illumination level may be modeled through the offset term, δc. The physical correctness and practical application advantages of model (2) have been shown in [7] and [8].

The first-order Taylor series expansion of the model (2) arrives at a constraint equation for computing optical flow:

$$E_t + E_x u + E_y v - Em_t - c_t = 0. \quad (3)$$

where $u = x_t = \lim_{\delta t\to 0}\delta x/\delta t$, $v = y_t = \lim_{\delta t\to 0}\delta y/\delta t$, $m_t = \lim_{\delta t\to 0}\delta m/\delta t$, and $c_t = \lim_{\delta t\to 0}\delta c/\delta t$.

III. LEAST SQUARES SOLUTION

In a small image region, neighboring points have similar velocities, with the exception of points near motion or depth discontinuity boundaries. Similarly, the brightness change fields vary slowly in most regions of the image, except near boundaries of reflectance or illumination discontinuities; i.e., cast shadows, etc. It can be assumed that the optical flow and brightness change fields are (approximately) constant within small image regions, which we take to be square windows of size $n \times n$ centered at each image point, for convenience. Therefore, a least squares formulation can be employed to estimate the four parameters u, v, m_t, and c_t at the center of the square:

$$\left[\sum \begin{pmatrix} E_x^2 & E_xE_y & -E_xE & -E_x \\ E_xE_y & E_y^2 & -E_yE & -E_y \\ -E_xE & -E_yE & E^2 & E \\ -E_x & -E_y & E & 1 \end{pmatrix}\right] \begin{pmatrix} u \\ v \\ m_t \\ c_t \end{pmatrix} = \sum \begin{pmatrix} -E_xE_t \\ -E_yE_t \\ EE_t \\ E_t \end{pmatrix}. \quad (4)$$

Provided that the 4×4 matrix is not singular, a solution can be derived in closed form. The solution of equation (4) requires the estimation of image gradients using finite difference methods. The commonly used $2 \times 2 \times 2$ templates (reference [9] chapter 12) for gradient estimation are

$$\begin{aligned} E_x &= [(1+\beta+\gamma+\beta\gamma)(\alpha-1)E]/4, \\ E_y &= [(1+\alpha+\gamma+\alpha\gamma)(\beta-1)E]/4, \\ E_t &= [(1+\alpha+\beta+\alpha\beta)(\gamma-1)E]/4. \end{aligned} \quad (5)$$

In equations (5), we use $Z-$transform-like operators α, β, γ. If $E \equiv E(i,j,k)$ is assumed to be the reference, $\alpha E \equiv E(i+1,j,k)$, $\beta E \equiv E(i,j+1,k)$, $\gamma E \equiv E(i,j,k+1)$, and so on. Cascading operations, such as $\alpha\beta E \equiv E(i+1,j+1,k)$ and $\alpha\gamma E \equiv E(i+1,j,k+1)$, are also allowed.

In order to eliminate the bias caused by phase shifting [7][8], we use an average brightness $\bar{E}$ in equation (4). The average version of the brightness is

$$\bar{E} = [(1+\alpha+\beta+\alpha\beta)(1+\gamma)E]/8. \quad (6)$$

By evaluating the coefficient matrices of equation (4) with these gradient estimates (and the average version of the brightness), we can obtain the brightness change fields m_t and c_t in addition to the two optical flow parameters u and v, if desired.

IV. ERROR ANALYSIS

The coefficients in equation (4) depend on the particular image being processed. To determine the general behavior of the solution, we may assume a statistical model for the image function, and approximate the summations in (4) using their expectations.

We assume that brightness E is a two-dimensional stationary random variable with mean M, and its spatial correlation function is

$$\mathcal{E}[E(x,y,t)E(x',y',t)] = (R_o^2 - M^2)e^{-\tau^2/D^2} + M^2, \quad (7)$$

where τ is the distance between the two image points, that is,

$$\tau = \sqrt{(x-x')^2 + (y-y')^2}.$$

R_o^2 is the auto-correlation of the brightness, and D^2 depends on the nature of the image. A large D^2 indicates that the image brightness is tightly correlated with its neighbors. Or, in other words, the image brightness is smooth. On the other hand, a very small D^2 (near zero) means that the image brightness is almost independent.

We further assume that the distances between two adjacent pixels along $x-$axis direction and along $y-$axis are both equal to d. Therefore, for example, the expectation

of the product of the brightness of two adjacent pixels along $x-$axis is

$$\mathcal{E}[E\alpha E] = (R_o^2 - M^2)e^{-d^2/D^2} + M^2.$$

Using the defined correlation function (7) to evaluate the coefficients of (4), we have:

$$\begin{pmatrix} a_{11} & a_{12} & 0 & 0 \\ a_{21} & a_{22} & 0 & 0 \\ 0 & 0 & a_{33} & a_{34} \\ 0 & 0 & a_{43} & 1 \end{pmatrix} \begin{pmatrix} \hat{u} \\ \hat{v} \\ \hat{m}_t \\ \hat{c}_t \end{pmatrix} = \begin{pmatrix} b_1 \\ b_2 \\ b_3 \\ b_4 \end{pmatrix}, \quad (8)$$

where, $\hat{u}, \hat{v}, \hat{m}_t$, and $\hat{c}_t$ are the parameters to be recovered. The expressions of these coefficients are very lengthy; for example,

$$\begin{aligned} a_{11} &= \frac{1}{8}(R_o^2 - M^2)[2(2 + 2m_t + m_t^2)(1 - e^{-2d^2/D^2}) \\ &\quad +(1 + m_t)(4e^{-(u^2+v^2)/D^2} + 2e^{-[u^2+(d+v)^2]/D^2} \\ &\quad +2e^{-[u^2+(d-v)^2]/D^2} - 2e^{-[(d+u)^2+v^2]/D^2} \\ &\quad -2e^{-[(d-u)^2+v^2]/D^2} - e^{-[(d+u)^2+(d+v)^2]/D^2} \\ &\quad -e^{-[(d-u)^2+(d+v)^2]/D^2} - e^{-[(d+u)^2+(d-v)^2]/D^2} \\ &\quad -e^{-[(d-u)^2+(d-v)^2]/D^2})], \\ a_{12} &= \frac{1}{8}(R_o^2 - M^2)(1 + m_t)(e^{-[(d+u)^2+(d+v)^2]/D^2} \\ &\quad -e^{-[(d-u)^2+(d+v)^2]/D^2} - e^{-[(d+u)^2+(d-v)^2]/D^2} \\ &\quad +e^{-[(d-u)^2+(d-v)^2]/D^2}), \\ b_1 &= \frac{1}{8}(R_o^2 - M^2)(1 + m_t)(2e^{-[(d+u)^2+v^2]/D^2} \\ &\quad -2e^{-[(d-u)^2+v^2]/D^2} + e^{-[(d+u)^2+(d+v)^2]/D^2} \\ &\quad -e^{-[(d-u)^2+(d+v)^2]/D^2} + e^{-[(d+u)^2+(d-v)^2]/D^2} \\ &\quad -e^{-[(d-u)^2+(d-v)^2]/D^2}) \end{aligned}$$

It is very difficult (if not impossible) to solve equation (8) for u and v in closed form. Therefore, we first discuss several special cases, then resort numerical computations.

1. No Motion If the actual motion $u = v = 0$, we find

$$a_{11} = \frac{1}{4}(R_o^2 - M^2)(2 + 2m_t + m_t^2)(1 - e^{-2d^2/D^2}),$$

$$a_{12} = b_1 = 0.$$

Because a_{11} is nonzero (except for images with uniform brightness, that is, $R_o^2 = M^2$), the solution is obviously

$$\hat{u} = 0$$

Similar result can be obtained for $\hat{v} = 0$. We would like to emphasize that this result is important since the solution could be biased [8] if care is not taken in the implementation of the algorithm.

2. Smooth Image and Small Motion Assuming the image is smooth and the motion is small, we have $d \ll D$, $u \ll D$, and $v \ll D$. Then, these lengthy expressions can be linearized using the approximation $e^x \approx 1 + x$: $a_{11} = \frac{1}{2}(R_o^2 - M^2)[d^2(2 + 2m_t + m_t^2) + 2d^2(1 + m_t)]/D^2$, $a_{12} = 0$, $b_1 = 2(R_o^2 - M^2)du(1 + m_t)/D^2$. Therefore, the estimated $\hat{u}$ is

$$\hat{u} = \frac{4du(1 + m_t)}{(2 + m_t)^2 d^2}. \quad (9)$$

A similar result can be obtain for $\hat{v}$, that is

$$\hat{v} = \frac{4du(1 + m_t)}{(2 + m_t)^2 d^2}. \quad (10)$$

It can be seen that $\hat{u} = u/d$ and $\hat{v} = v/d$ when the brightness change field $m_t = 0$. The recovered motion is in the form of the fraction of the pixel size d as expected. When m_t is not zero, the results are biased. However, the sign of u and v will not be reversed since $-1.0 < m_t < +\infty$. This is also an important finding which leads to use of the iterative shifting algorithm described in section V of this paper.

3. Numerical Evaluation For general cases, we resort numerical computations. Two sets of experiments are used to verify our modeling and analysis. Fig. 1(a) is a random image generated by computer and its measured correlation function is shown in Fig. 1(b). Based on the measured data, the correlation function is obtained by minimizing the error:

$$\sum [R(\tau^2) - (R_o^2 - M^2)e^{-\tau^2/D^2} + M^2]^2. \quad (11)$$

For this random image, we obtained $D = 4.08(d)$, where d is the pixel size in 512 x 512 images. In Fig. 1(b) the scattering marks are the measured data points and the solid line is the fitted curve with $D = 4.08$. Experiments are first performed for various u with $v = 0.5$ and $m_t = 0$, In Fig. 1(c) the solid diagonal line is the actual u. The dashed line indicates the data from optical flow computations, and the dotted line shows the results from our analysis. It can be seen that the analyzed results are very close to the data from optical flow computations. The maximum differences at $u = 1$ and $u = -1$ are less than 10 percent. Another experiment is performed for various u but $v = 0.5$ and $m_t = -0.3$. The analyzed data are still very close (within 10 percent) to the real optical flows. (Results are not illustrated in this paper.)

Fig. 2(a) is a real image of the book cover of *Robot Vision*. It is much smoother than Fig. 1(a). Based on the similar measurements to Fig. 1(b), the correlation parameter $D = 20(d)$ is obtained using (11). Experiments with various u but $v = 0.5$ and $m_t = 0$ (or $m_t = -0.3$) are also performed on these images. The results with $m_t = -0.3$ are shown in Fig. 2(b). It can be seen that the error is much smaller than that from image 1(a). In all cases, the analyzed error almost coincides with the real optical flow data.

Error Characteristics

Based on our analysis and experiment results we can make several conclusions about the error in optical flow computations.

1. Optical flow from smooth images (brightness is highly correlated with its neighbors) has less error. Zero error could be assumed with very smooth[1] images ($d \ll D$) and null brightness change field.

[1] Notice that optical flow computation will fail for images with uniform brightness because spatial gradients are all zero there.

2. Generally, with nonzero brightness changes optical flow is erroneous except for $u = v = 0$.
3. The erroneous optical flow always has the same sign of the actual flow no matter how the brightness changes.

V. ITERATIVE SHIFTING ALGORITHM

Based on the error analysis, we developed an iterative shifting algorithm to determine optical flow (horizontal motion) accurately. The basic idea behind the algorithm is to utilize the facts that erroneous optical flow remains the same sign as the actual flow and zero motion can be determined without errors. In order to perform the algorithm, image frames are stored on computer with two different formats: full-size 512 × 512 8-bit images and reduced-size 64 × 64 floating point numbers. Each pixel in a reduced-size image is an average of 8 × 8 pixels of its corresponding full-size image.

Suppose a pair of images A and B is used to determine the horizontal motion. The steps to perform the algorithm are

1. Setting initial values of the two motion parameters $u = 0$ and $v = 0$. Reducing full-size image A to reduced-size image a.
2. Reducing full-size image B to reduced-size image b.
3. Performing optical flow computation on a and b, that is, using equation (4), the gradient estimates (5), and the average brightness (6), to obtain the estimated motion parameter $\hat{u}$ and $\hat{v}$.
4. Checking whether the absolute values of $\hat{u}$ and $\hat{v}$ are both smaller than a predetermined threshold; if yes, go to step 10, else continue. We use 0.06 as the threshold which is equivalent to $0.06 \times 8 = 0.48$ pixels in the full-size image.
5. Converting the estimated $\hat{u}$ and $\hat{v}$ to full-size image scale, for example, in our cases, computing $\hat{u}_f = 8 \times \hat{u}$ and $\hat{v}_f = 8 \times \hat{v}$.
6. Rounding up $\hat{u}_f$ and $\hat{v}_f$ to integers, that is, $\hat{u}_i = (integer)\hat{u}_f$ and $\hat{v}_i = (integer)\hat{v}_f$.
7. Shifting image B by $-\hat{u}_i$ along $x-$axis and $-\hat{v}_i$ along $y-$axis.
8. Accumulating the recovered motion $u = u + \hat{u}_i$ and $v = v + \hat{v}_i$.
9. Going back to step 2.
10. Ending the computation. The results are u and v.

The suggested method is similar to correlation methods in the sense of looking for best match between two images. However, the advantages of using the proposed method are significant with respect to speed and robustness.

Speed Advantage In correlation methods, blind searching a neighbor region for best match is lengthy. In the proposed method, the searching direction and the amount for shifting are approximately correct. Therefore, the proposed method is much more efficient. For example, assume that the maximum motion between two successive image frames is 10 pixels in 512 × 512 images. Correlation requires at least $10 \times 10 \times 512 \times 512 \approx 25$ million multiplications and $10 \times 10 = 100$ comparisons. Using the proposed optical flow, the computation is about 786 thousand ($3 \times 512 \times 512$) additions and 16 thousand ($4 \times 64 \times 64$) multiplications. The speed advantage has been verified by real image computations, an example will be shown in section VI.

Robustness Advantage Since the iterative shifting method employs the generalized brightness model allowing brightness changes among image frames, it is more robust than correlation methods. With brightness changes, for example, in Experiment 2 (described in the next section) the correlation method fails (giving wrong results $u = v = 0$), but the suggested method still provides accurate results.

VI. SELECTED EXAMPLES

Experiments using real image with real motion are performed to test the accuracy and robustness of the suggested method.

Example 1. Two images from the sequence of the book cover "Robot Vision" Fig. 2(a) are used for this experiment. The actual motion is $u = -8$ and $v = 0$. The results obtained from the proposed method and correlation are shown below.

	proposed	correlation
recovered motion $\hat{u} =$	-8	-7
recovered motion $\hat{v} =$	-1	0
time on DEC5000/133	22"	4'50"
time on HP9000/300	4'4"	22'6"

Example 2. A pair of underwater images are used for this experiment. Due to back-scattering, the dynamic range of the image brightness is quite narrow. Fig. 3 shows the brightness histograms of the pair of images. The brightness changes can also be seen in the histogram. The actual motion is $u = 8$, $v = 3$ and the recovered parameters are $\hat{u} = 8$ and $\hat{v} = 3$. The correlation method fails in this instance giving $u = v = 0$.

Example 3. A sequence of four underwater images (#1 - #4) is used for motion recovery, one of them is shown in Fig. 4(a). There are motions as well as brightness changes among these images. Three different paths are used for the motion (optical flow) computation. They are #1 - #2 - #3 - #4, #1 - #3 - #4, and #1 - #4. We expect that the same final position will be reached with different paths if optical flow computations are accurate.

When the obtained optical flows are directly used, the results shown in Fig. 4(b) are obtained. The differences between results from different paths are too large to be acceptable. For example, the path #1 ~ #4 gives the final position $(-6, -6)$ which is considerably removed from the actual position $(-9.5, -9.5)$. Fig. 4(c) shows the results from the iterative shifting method, the differences of the final positions are less than a single pixel.

VII. SUMMARY

Although many developed techniques have been used for underwater stationkeeping and/or navigation, detection of slow horizontal motion is still a difficult task. In this paper, we have proposed an optical sensing method based on optical flow computations for horizontal motion recovery.

We first treated the image brightness as a spatial random variable and employed correlation functions to describe solutions for motion based on optical flow computations. We performed an error analysis and found error expressions for the general case with brightness

changes which cannot be modeled by brightness constancy. Through our error analysis and real image experiments, we concluded that optical flow is erroneous except for zero motion. However, we also found that the erroneous flow always has the same sign as the actual flow. Based on these findings we developed an algorithm to determine accurate motion between two image frames. This method is similar to correlation methods attempting to match two images; however, optical flows are used instead in the matching process. In opposition to correlation methods, the best matching is not determined by a maximized correlation measure but determined by a zero optical flow, from which a much faster and more robust solution can be obtained as evidenced by our experiments.

It should be noted that the developed method assumes that the rotational motion of the subsea vehicle is determined by other means such as gyroscopes and that the depth change is detected by pressure sensors. Our further research will address the coordination of six-freedom motion determination for stationkeeping and/or navigation.

Many applications require the development of intelligent/autonomous subsea vehicles and certainly accurate positioning and localization are necessary capabilities for these vehicles. Our research suggests an optical sensing and computing technique to achieve these capabilities.

REFERENCES

1 B.K.P. Horn and B.G. Schunck, "Determining Optical Flow," *Artificial Intelligence*, vol. 17, 1981.

2 S.Q. Duntley, "Light in the Sea," *Journal of Optical Society of America*, Vol.53, 1963.

3 L. E. Mertens, *In Water Photography: Theory and Practice*, Wiley–Interscience, New York, N. Y. 1970.

4 N. Cornelius and T. Kanade, "Adapting Optical Flow to Measure Object Motion in Reflectance and X-Ray Image Sequence," ACM SIGGRAPH/SIGART *Interdisciplinary Workshop on Motion: Representation and Perception*, Toronto, Canada, April, 1983.

5 N. Mukawa, "Motion Field Estimation for Shaded Scenes," *International Conference on Image Processing*, Singapore, September,1989.

6 S. Negahdaripour, A. Shokrollahi, and M. Gennert, "Relaxing the Brightness Constancy Assumption in Computing Optical Flow," *International Conference on Image Processing*, Singapore, September,1989.

7 S. Negahdaripour and C.H. Yu, "A Generalized Brightness Change Model for Computing Optical Flow," *International Conference on Computer Vision*, Berlin, Germany, May, 1993.

8 S. Negahdaripour and C.H. Yu, "Computing Optical Flow for Scenes with Time-Varying Brightness," submitted to IEEE Trans. on PAMI.

9 B.K.P. Horn, *Robot Vision*, MIT Press, Cambridge, Massachusetts, 1986.

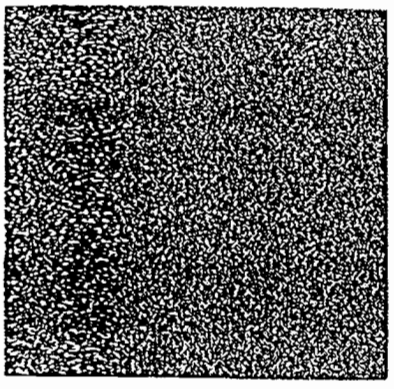

(a) A Random Image

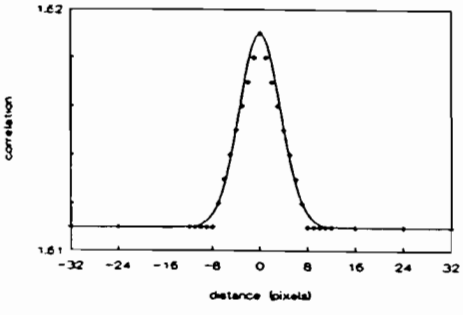

(b) Brightness Correlation Function

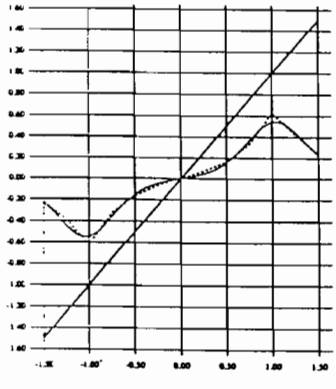

(c) Result Comparison

Figure 1. Numerical computations are performed on a random image (a) to verify the error analysis. In (b), the scattered marks are correlation measurements and the solid line is the fitted curve (to obtain D). In (c), the results from the analysis are shown with dotted line, the optical flow data — dashed line, and the actual parameter — solid line.

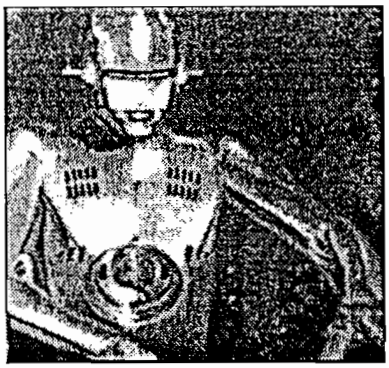

(a) Image of Book Cover of "Robot Vision"

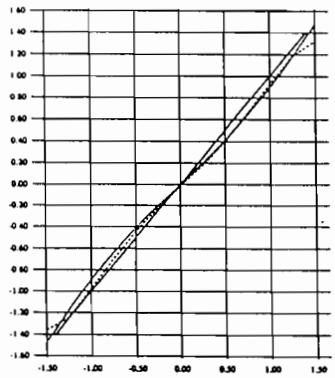

(b) Result Comparison

Figure 2. Numerical computations are performed on image (a) to verify the error analysis. In (b), the results from the analysis are shown with dotted line, the optical flow data — dashed line, and the actual parameter — solid line.

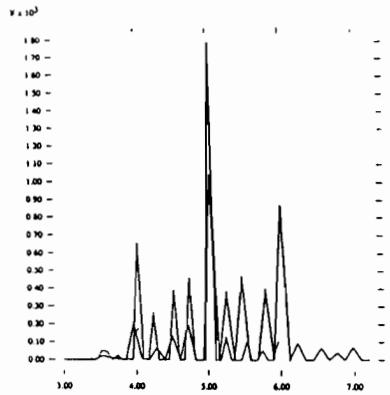

Brightness Histogram

Figure 3. A pair of underwater images (not shown) is used in Example 2. The brightness histogram of the two images shows that the narrow brightness dynamic range and brightness changes. Correlation fails for the two images but the proposed method still provides accurate results.

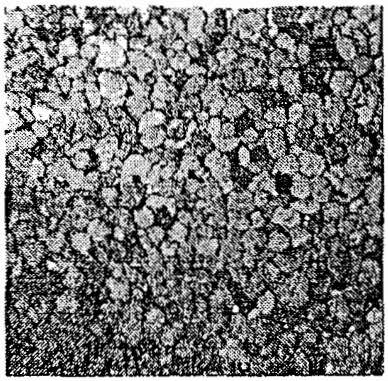

(a) An Underwater Image

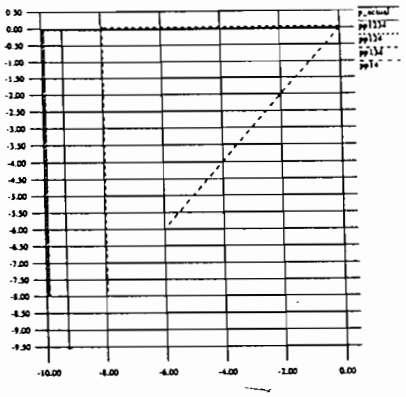

(b) Results from Optical Flow

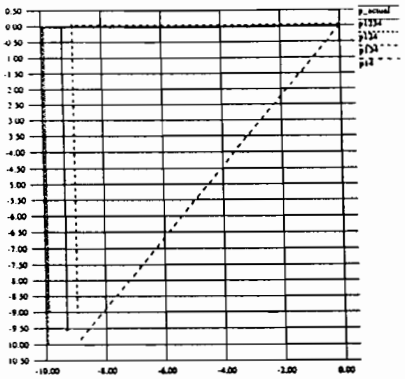

(c) Results from Proposed Method

Figure 4. A sequence of four images is used for Example 3. An image in the sequence is shown in (a). It can be seen in (b), optical flow from different paths provides results removed from each other. Results from the proposed method are shown in (c). The errors are less than a single pixel.